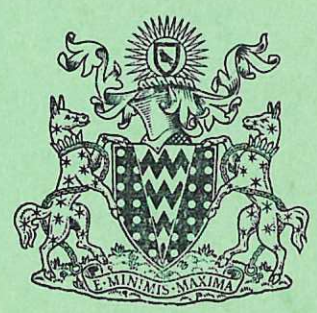

United Kingdom Atomic Energy Authority

RESEARCH GROUP

Preprint

THE ENERGY SPECTRA OF THE NEUTRONS FROM ZETA

R. A. COOMBE

B. A. WARD

Culham Laboratory,

Culham, Abingdon, Berkshire

1963

UNCLASSIFIED
(Approved for Publication)

CLM - P 21

THE ENERGY SPECTRA OF THE NEUTRONS FROM ZETA

by

R. A. COOMBE*

B. A. WARD

(Submitted for publication in Journal of Nuclear Energy, Part C.)

ABSTRACT

The energy of neutrons emitted tangential and perpendicular to the discharge axis of ZETA has been measured using a hydrogen-filled diffusion cloud chamber. Several different discharge conditions were studied.

The results are consistent with the conclusions of other workers that the neutron emission is due to a small number of high-energy deuterons. In addition, analysis of the shape of the neutron spectra suggests the possibility that the deuterons have a velocity which is predominantly perpendicular to the gas current axis and that they travel in a helix with energies up to 350 keV.

*Reactor Physics Department, University of Birmingham.

U.K.A.E.A. Research Group,
Culham Laboratory,
Nr. Abingdon,
BERKS.

March, 1963
(C 18) /ED

C O N T E N T S

T A B L E S

1. INTRODUCTION

1. The presence of high-energy ordered ion motion in toroidal pinch discharges was first demonstrated by ROSE et al. (1958) in ZETA (BUTT et al., 1958; MITCHELL et al., 1959). Their results indicated that the neutrons came from fusing deuteron pairs whose centre-of-mass had a velocity component of 6×10^7 cm/sec in the direction of positive gas-current. Analysis of the neutron energy spectrum from the Perhapsatron (CONNER et al., 1958) and the proton energy spectrum from Sceptre (HUNT,1960; JONES et al.,1961) has yielded similar results. The nature of the acceleration mechanism responsible for this ordered motion is not understood. The present experiments were designed to obtain further information on the magnitude and direction of the accelerating force by measuring the components of centre-of-mass velocity of the fusing deuterons tangential and perpendicular to the discharge axis*, and observing the change in these quantities with different discharge conditions of ZETA.

2. A diffusion cloud chamber was used to determine the neutron energy spectra. In the first place, the measurements of ROSE et al. (1958) were repeated but with some differences:

(a) Deuterons emitted in two opposite directions tangential to the discharge axis were examined by changing the direction of observations of the cloud chamber rather than by reversing the gas current direction.

(b) The potential of the condenser bank and hence the gas current was increased slightly, as were the gas pressure and applied axial magnetic field, to take advantage of the consequent increase in neutron yield.

(c) Certain structural changes had been made to ZETA, in particular the installation of a continuous corrugated stainless steel torus liner in place of the insulated segments and a rearrangement of the axial magnetic field coils, resulting in a more uniform field.

Secondly, measurements were made on ZETA 3MJ (MITCHELL et al., 1959) where the increase in gas current up to 500 kA gave a neutron yield sufficiently high to make possible observation of the spectra of neutrons emitted perpendicular to the discharge axis.

---

* In order to avoid confusion which sometimes arises when speaking of the axis of a torus, the term 'discharge axis' is used throughout, this being the locus of the centres of circles obtained by taking vertical cross sections of the ZETA discharge tube.

2. EXPERIMENTAL DETAILS

GENERAL ARRANGEMENT

3. The position of the cloud chamber relative to ZETA is shown in Figure 1. The cloud chamber was placed in position 1 to observe neutrons emitted tangential to the discharge axis and in position 2 to observe neutrons emitted perpendicular to the discharge axis. A stainless steel tank filled with water (4) was used as the main neutron shield and collimator. The thickness of water interposed between the torus and the cloud chamber (27 inches) was sufficient to ensure that less than 5 per cent of the neutrons detected originated outside the volume of the ZETA discharge viewed by the collimating aperture. The cloud chamber (3) was mounted on a turntable in a cavity in the tank and could be rotated to view different parts of the discharge. An auxiliary collimator (5) of paraffin wax blocks could be arranged to define the view without moving the tank. The approximate position of the gas discharge channel (6) the iron transformer core (7) and the one inch thick aluminium torus (8) are also shown in Figure 1. A sheet of lead, $\frac{1}{4}$ inch thick, was placed in the path of the neutrons to attenuate the X-rays emitted by the discharge which would otherwise have depleted the sensitive layer of the cloud chamber.

THE CLOUD CHAMBER

4. Neutron energy was measured by observing the range and scattering angle of the protons produced by elastic n-p scattering in hydrogen in the sensitive layer of a cloud chamber. The cloud chamber (BATSON et al., 1956), kindly lent by Birmingham University, was designed for use with gas pressures up to 25 atmospheres. For the present experiments a pressure of 10 atmospheres of hydrogen was used, this being a compromise between detection efficiency, which is proportional to pressure, and accuracy of track measurement, which is proportional to particle range and hence inversely proportional to gas density. Optimum track formation was obtained with a base temperature of approximately -53°C and a temperature gradient across the sensitive layer of 5.5°C/cm. The vapour trails (methanol) produced by the protons were allowed to develop for at least 80 ms before being photographed by a stereoscopic camera.

CALIBRATION

5. The stopping power of the sensitive layer of the cloud chamber was determined with the aid of a pulsed d-d neutron source of the type described by HAWKINS and SUTTON (1960). The neutrons emitted perpendicular to the direction of acceleration of the ions in this

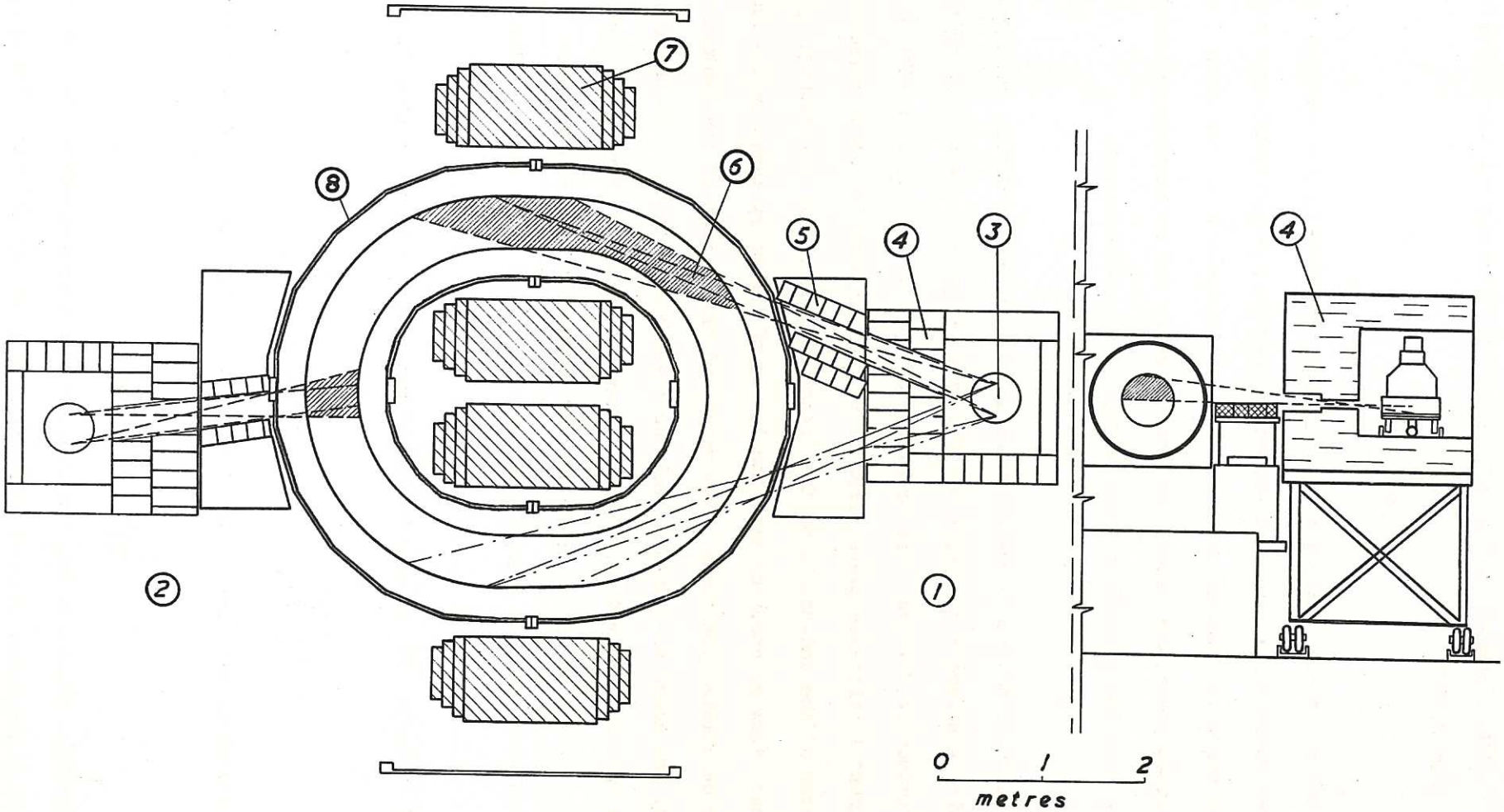

CLM-P 21 Fig. 1 Alternative positions of the cloud chamber relative to ZETA.

tube have an energy of 2.46 MeV. A neutron of energy E_n, when scattered from a hydrogen atom in the cloud chamber, ejects a proton of energy E_p, at an angle ψ to the initial neutron direction such that:-

$$E_p = E_n \cos^2 \psi \qquad (1)$$

6. The range R and scattering angle ψ of the protons, produced by the neutrons of known energy from the d-d tube source, gave the proton range-energy relationship appropriate to the gas density in the cloud chamber sensitive layer. Calibration of the cloud chamber to obtain this relationship was performed at intervals during the experiments and demonstrated a drift of less than 50 keV (neutron energy) over a 12 hour run.

TRACK MEASUREMENT

7. The proton tracks in the cloud chamber were up to 5 cm long and were photographed by a double camera with a stereoscopic angle of 12°. The ranges and scattering angles of the protons were determined as follows. The tracks were reprojected, for each stero-view in turn, onto a horizontal reference plane parallel to the image of the cloud chamber base and the co-ordinates of the end-points of the tracks recorded. The co-ordinate system was aligned for each view by ensuring that the images of fiduciary marks in the chamber appeared at their calculated positions. The range and orientation of the protons were then computed from the above co-ordinates and the measured constants of the system such as image distance and lens separation. The calculations included corrections for obliquity of the tracks in the sensitive layer and the consequent pressure gradient encountered, and gave the neutron energies and an estimate of their standard deviation.

ERRORS

8. The standard deviation ΔE_n in neutron energy measured by the above procedure is given by:-

$$\Delta E_n = \left[\left[\frac{\delta E_n}{\delta E_p} \cdot \Delta E_p \right]^2 + \left[\frac{\delta E_n}{\delta \psi} \cdot \Delta \psi \right]^2 \right]^{\frac{1}{2}}$$

where ΔE_p is the standard deviation in the measurement of E_p and $\Delta\psi$, the error in ψ. Since:-

$$\frac{\delta E_n}{\delta \psi} = 2 E_n \tan \psi$$

ΔE_n is a function of ψ. Values of ΔE_n computed for the tracks observed are almost uniformly distributed in frequency between energies of 200 keV and 800 keV. The largest

contribution to the error is $\Delta\psi$, this being the resultant of errors in measurement of the track co-ordinates and the 3° half-width of the neutron collimator.

9. Uncertainty in the depth of the end-points of the track in the chamber, due to the small stereoscopic angle used, also makes a large contribution to the total deviation. The position co-ordinates of the reprojected tracks were measured with an estimated standard deviation of 0.2 mm. For a typical track (R = 3.64 cm, $\psi = 12.8^{\circ}$) this gave a standard deviation in range of 2 per cent. The total deviation ΔE_n for this track was 3.6 per cent, the resultant of 3.3 per cent from scattering angle deviations, 1 per cent from standard deviations in calibration of the sensitive layer and 1 per cent from deviations in range measurement.

THE EXPERIMENTS

10. Two separate experiments were carried out. In experiment 1 the spectrum of neutrons emitted in two opposite directions tangential to the discharge axis of ZETA 1A was measured. The 0.5 MJ condenser bank was charged to its maximum working potential of 24 kV. This produced a peak gas current $\hat{I}_g$ of 280 kA. To maintain a magnetic field configuration similar to that of the discharge investigated by ROSE (1958) the parameter $\hat{\theta}$ was kept at 4.2 by applying an initial axial magnetic field B_{zo} of 270 gauss. $\hat{\theta}$ denotes the maximum compression produced by the magnetic field for an idealised pinch system and is defined by:-

$$\hat{\theta} = 2\,\hat{I}g/aB_{zo},$$

a being the discharge tube radius. The initial gas pressure was 0.3 m torr, this being the pressure which gave the maximum neutron yield.

11. Experiment 2, performed on ZETA 3 MJ, was more complex. During a survey of neutron yield versus applied axial magnetic field to determine the discharge conditions for maximum yield, two distinct types of discharge were observed for apparently identical initial conditions. Some discharges were characterised by a reproducible, smoothly varying, high-current waveform with low electrical resistivity at peak current and moderate X-ray and neutron yields. With approximately equal frequency and alternating randomly with the above discharge type, discharges occurred with low, non-reproducible current waveforms and exhibiting relatively high resistivity, neutron and X-ray yields. Typical oscilloscope traces of the current waveform and neutron rate-meter output for the two types

of discharge are shown in Figure 2. By taking photographs of the cloud chamber tracks after each discharge it was possible to construct the energy spectra of neutrons emitted by both types of discharge. The results relating to the high current type of discharge are referred to as 'Experiment 2α' the results of the low current discharge as 'Experiment 2β'.

12. These two types of discharge are due to the 'pumpout' phenomenon (BERNSTEIN et al., 1957). The initial discharge conditions are found to be those for which the consequent rate of loss of ions is sufficient to reduce the line density of the gas to the critical density value at an early stage during the discharge pulse (BURTON and WILSON, 1961; BURTON et al., 1961). A small variation in the rate of injection of ions into the plasma can thus have a considerable effect on the discharge characteristics; an injection rate sufficient to keep the line density above its critical value of about $6 \times 10^{16} cm^{-1}$ results in the α discharge. In the β discharge a lower injection rate enables the line density to fall to the point where electron runaway can occur, energy is lost from the plasma and the X-radiation is enhanced (GIBSON and MASON, 1961). The α discharge is the condition for which most of the confinement studies have been carried out.

13. The neutrons emitted perpendicular to the discharge axis were examined in two separate groups, namely those emitted from the top and bottom halves of that part of the discharge viewed by the collimator. These views were obtained by moving the paraffin wax blocks of the collimator and were intended to detect azimuthal motion of the deuterons. The main parameters of the ZETA discharge employed for the two experiments are listed in Table 1. (page 10).

3. RESULTS

TANGENTIAL SPECTRA

14. The spectra of neutrons emitted tangentially at 0° and 180° to the discharge axis are shown in Figures 3a and 4. The spectrum of neutrons emitted by the d-d tube is shown in Figure 3b. The histograms show the numbers of tracks giving neutron energies falling in 100 keV energy intervals. The smooth curves were obtained by addition of Gaussian profiles, as explained below. In Table 2 are summarised the main properties of these spectra, column 3 giving the weighted means and standard deviations of the mean of each spectrum derived from the computed values of E_n and ΔE_n, column 4 the standard deviations for each energy distribution, computed from E_n alone, and column 5 the difference between the weighted means of the 0° and 180° views of each experiment.

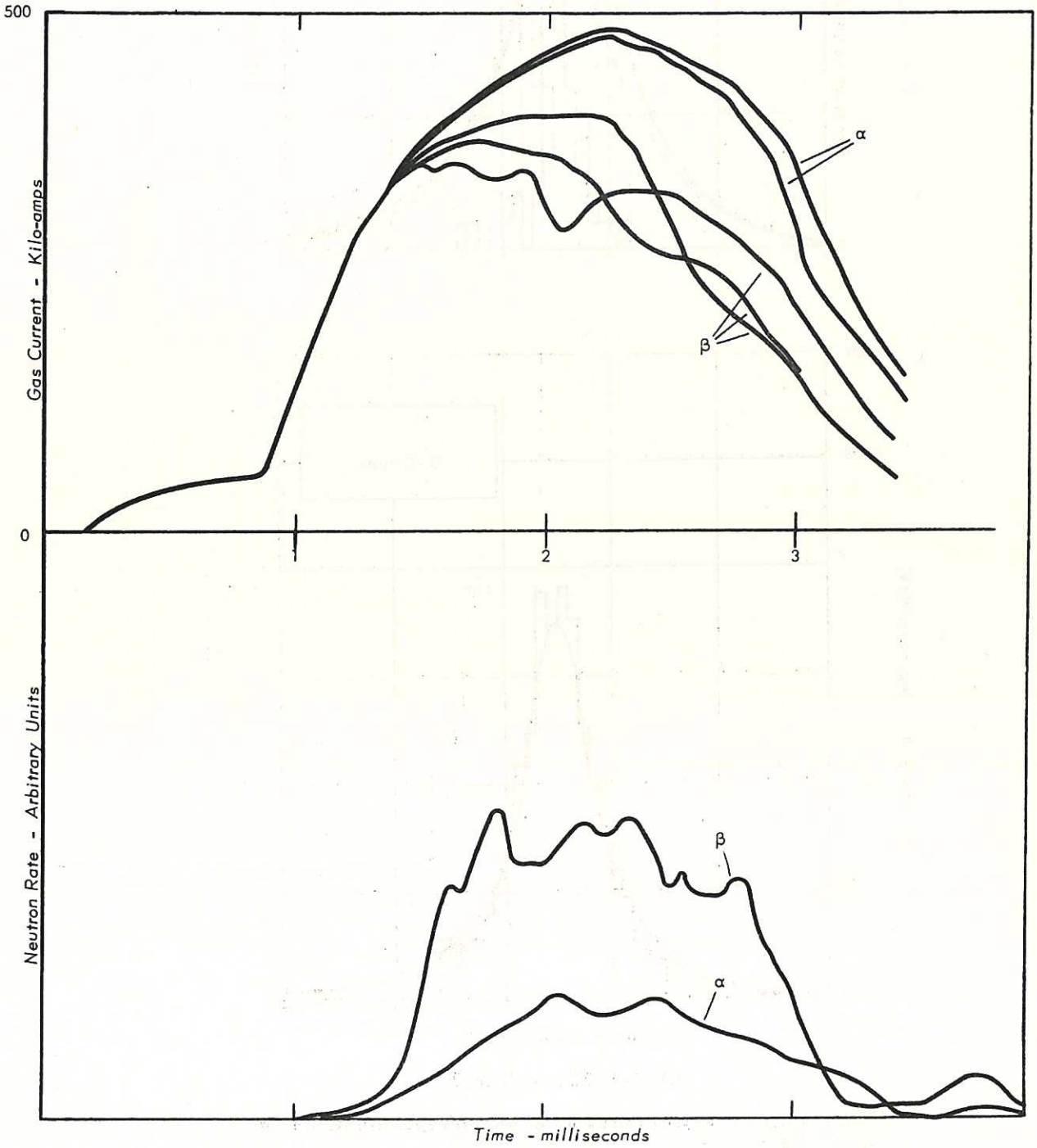

CLM-P 21 Fig. 2

The variation of gas current and rate of emission of neutrons with time from ZETA 3MJ under the conditions of Experiment 2. The traces given by the α and β discharges are shown.

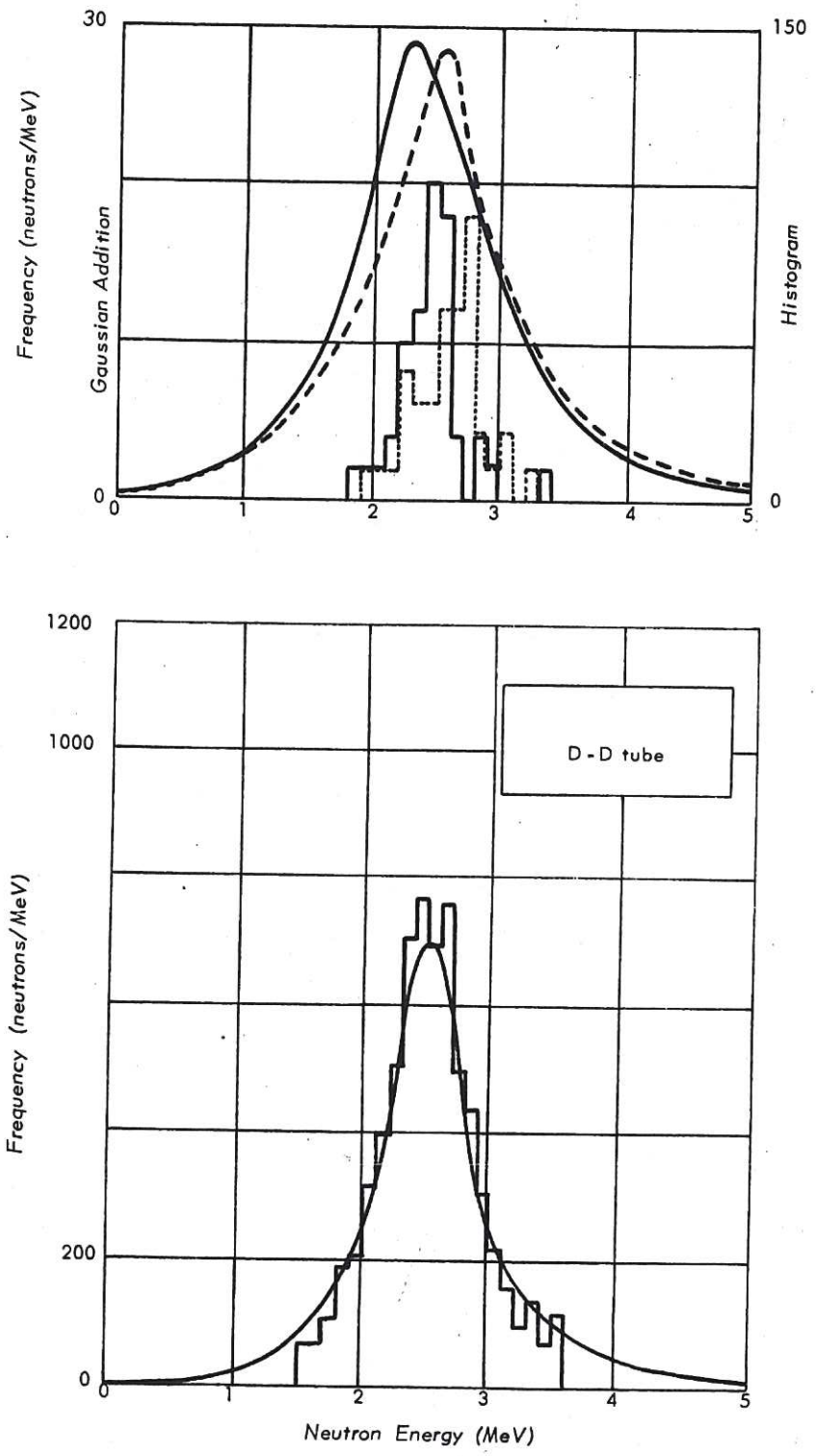

CLM-P 21 Fig. 3

The results of the two methods of spectra constructions are shown for

(a) The tangential spectra of neutrons emitted parallel (0°) and antiparallel (180°) to the direction of positive gas current (I_z) in ZETA during experiment 1.

(b) The observed energy spectrum of neutrons emitted from the d-d tube shielded with one inch of aluminium.

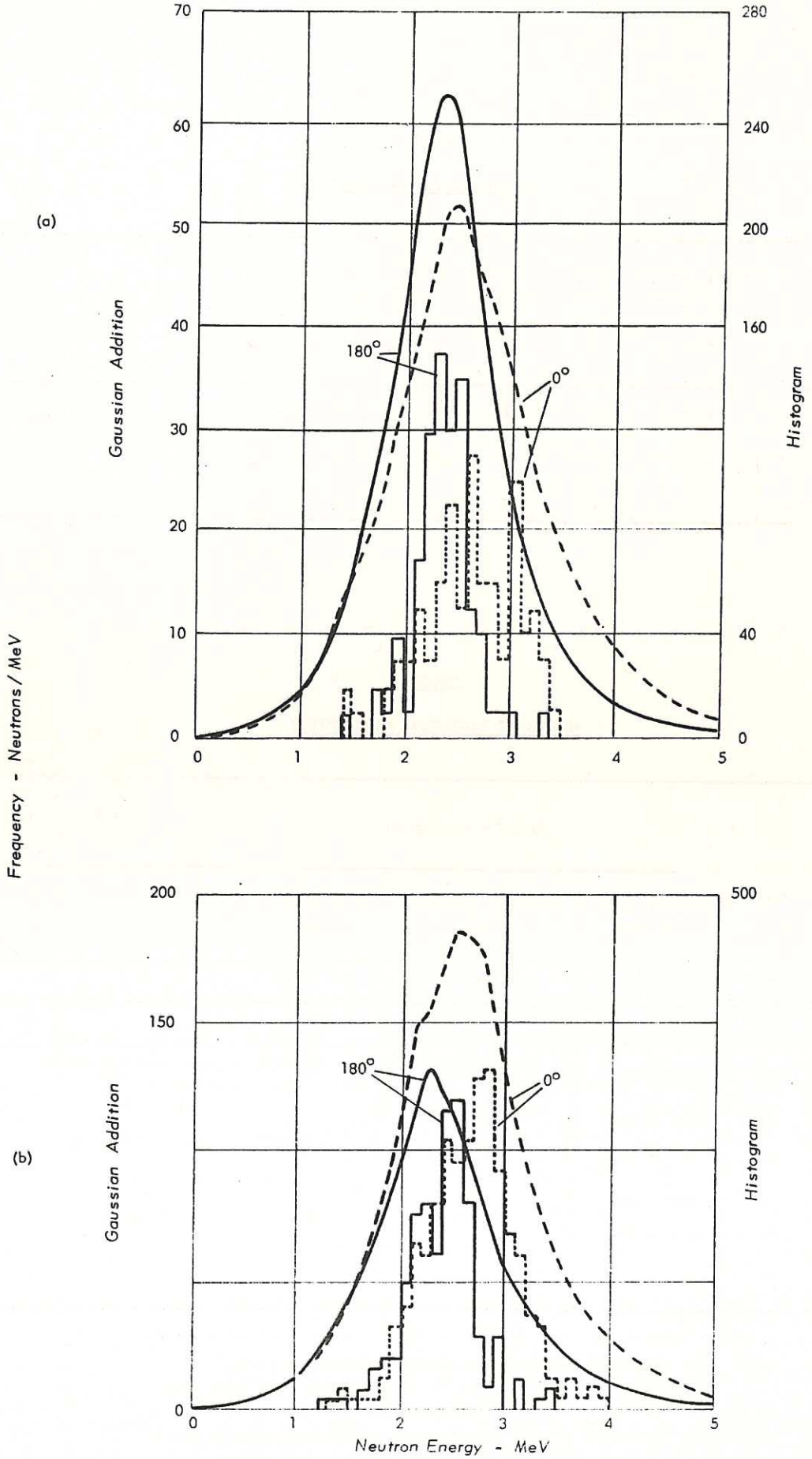

CLM-P 21 Fig. 4

The tangential spectra of neutrons from ZETA emitted parallel (0°) and antiparallel (180°) to the current axis (a) in Experiment 2α, and (b) in Experiment 2β.

TABLE 1.

EXPERIMENTAL CONDITIONS

Experiment	Machines	Energy stored in capacitor bank (M Joules)	Capacitor bank potential (kV)	Transformer turns ratio	Peak gas current I (kA)	Applied axial magnetic field B_{zo} (gauss)	Initial deuterium gas pressure (m torr)	$\hat{\theta} - \frac{\hat{I}}{25B_{zo}}$	Approximate total Neutron yield (number/discharge)
1	Zeta 1A	0.46	24	8:1	280	270	0.30	4.2	4×10^6
2α	Zeta 3MJ	1.08	15	4:1	500	1,100	0.25	1.8	1×10^7
2β	Zeta 3MJ	1.08	15	4:1	400-480	1,100	0.25	1.4-1.7	5×10^7

TABLE 2.

RESULTS OF TANGENTIAL MEASUREMENTS

Experiment	View*	From the histograms			From the Gaussian Addition Spectra	
		Weighted mean of neutron energy (MeV)	Standard deviation of the distribution (MeV)	Separation of the weighted means of the views (keV)	Separation of modes (keV)	Width at half height W (MeV)
1	0°	2.50 ± 0.07	0.24 ± 0.04	170 ± 90	220 ± 120	1.19 ± 0.13
	180°	2.33 ± 0.06				
2α	0°	2.34 ± 0.04	0.34 ± 0.03	30 ± 60	100 ± 80	1.24 ± 0.10
	180°	2.31 ± 0.04				
2β	0°	2.49 ± 0.02	0.32 ± 0.02	240 ± 30	250 ± 60	1.35 ± 0.06
	180°	2.25 ± 0.02				
Calibration	-	-	0.36 ± 0.02	-	-	0.80 ± 0.04

* Angle between directions of neutron emission and positive gas current.

15. These results based on histograms are open to the objection that a neutron energy spectrum obtained with a cloud chamber does not exhibit a Gaussian distribution of errors as the standard deviation in measurement is not constant but depends on angle (Paras.8,9). Moreover, a simple frequency histogram of the results does not use all the information available since the standard deviation ΔE_n of an observation can also be estimated. Continuous spectra were therefore constructed (see Figure 3 and 4) by assuming each track to give a neutron energy with a Gaussian probability distribution centred at the measured energy, enclosing unit area and with standard deviation equal to the computed deviation ΔE_n. The height of the profile from this event is thus inversely proportional to ΔE_n. The final energy spectrum intensity $f(E_i)$ is the sum of the individual profiles at energy E_i.

$$f(E_i) = \sum_{j=1}^{m} \frac{1}{(2\pi)^{\frac{1}{2}} \cdot \Delta E_j} \cdot \exp\left(\frac{-(E_i - E_j)^2}{2(\Delta E_j)^2}\right.$$

where m is the number of proton tracks recorded giving energies E_j with standard deviation E_j; the area under the final spectrum is proportional to the number of events contributing to it. This 'Gaussian Addition' construction gives the probability distribution of neutron energy in each experiment. The results from these distributed spectra are also given in Table 2. Column 6 gives the separation of the modes of the spectra together with their estimated standard deviations; the latter are calculated from the formula for the separation of the means of two Gaussian distributions, i.e:-

$$\text{standard deviation} = \sigma_d[(1/m_1) + (1/m_2)]^{\frac{1}{2}}$$

where m_1 and m_2 are the numbers of tracks observed at 0° and 180° respectively and σ_d is the standard deviation of a single determination derived from the width at half height of the 'Gaussian Addition' spectra. The last column of Table 2 gives the width at half height (W) of the sum of the 0° and 180° spectra, the standard deviation in this case being taken as:-

$$W \cdot (m_1 + m_2)^{-\frac{1}{2}}$$

16. The histograms were constructed for neutrons giving proton scattering angles ψ less than 40°. This restriction was relaxed for the Gaussian addition construction, scattering angles up to 60° being accepted.

ANALYSIS OF TANGENTIAL SPECTRA

17. It can be seen from Table 2 that in the experiments 1 and 2β a neutron energy

anisotropy is observed along the discharge axis, of which the simplest explanation, in accordance with the findings of previous workers (JONES et al., 1961; HERDAN and HUGHES, 1961; MATHER and WILLIAMS, 1958; ROSE et al., 1958; HUNT, 1960), is that deuterons are accelerated along the axis to energies of the order of 10 keV. A much lower anisotropy is observed in experiment 2a.

18. The Gaussian addition results have been interpreted, in the first place, in terms of a model in which the reacting deuteron pairs all have the same tangential component of centre-of-mass velocity (one-group model). For a larger number of values of centre-of-mass velocity, the expected neutron spectra were calculated, using the instrumental width of Figure 3b, and compared with the observed spectra by the method of least squares. The numerical work was performed on an IBM 7090 computer. The values which give the best fit are listed in Table 3, columns 2-7, and the spectra for these values are shown superimposed on the observed spectra in Figure 5.

19. Analysis was also carried out in terms of a two group model. It can be seen from Figure 5 that the one-group model does not give a very good fit to the data and moreover, examination of Figures 3 and 4 shows a systematic difference in shape between the 0° and the 180° spectra, in that the high-energy tails of the latter fall more slowly than those of the former, while the converse is true of the low-energy tails. The analysis for the two-group model was carried out in the same way as for the one-group model and the velocities giving the best fit are listed in Table 3, columns 8-13. The calculated spectra are also superimposed on the observed spectra in Figure 5.

20. The errors given in Table 3 were derived using the fact that the rate at which the sum of the squares of the differences between the ordinates of the experimental and model curves approaches a mimimum, as the relevent neutron energy is varied, defines the accuracy of the energy obtained by this method. The standard deviations given in Table 3 were calculated by finding the change in energy necessary to increase the sum of the squares of the residuals by a factor:-

$$\nu^{-1}\ \chi^2\ (0.70,\nu)$$

above the value at mimimum (COOPER, 1962 unpublished). ν is the number of degrees of freedom of the model under test (ν is decreased by 2 when the number of groups in the model is increased by one) and $\chi^2\ (0.70,\nu)$ is the value of the χ^2 distribution giving a

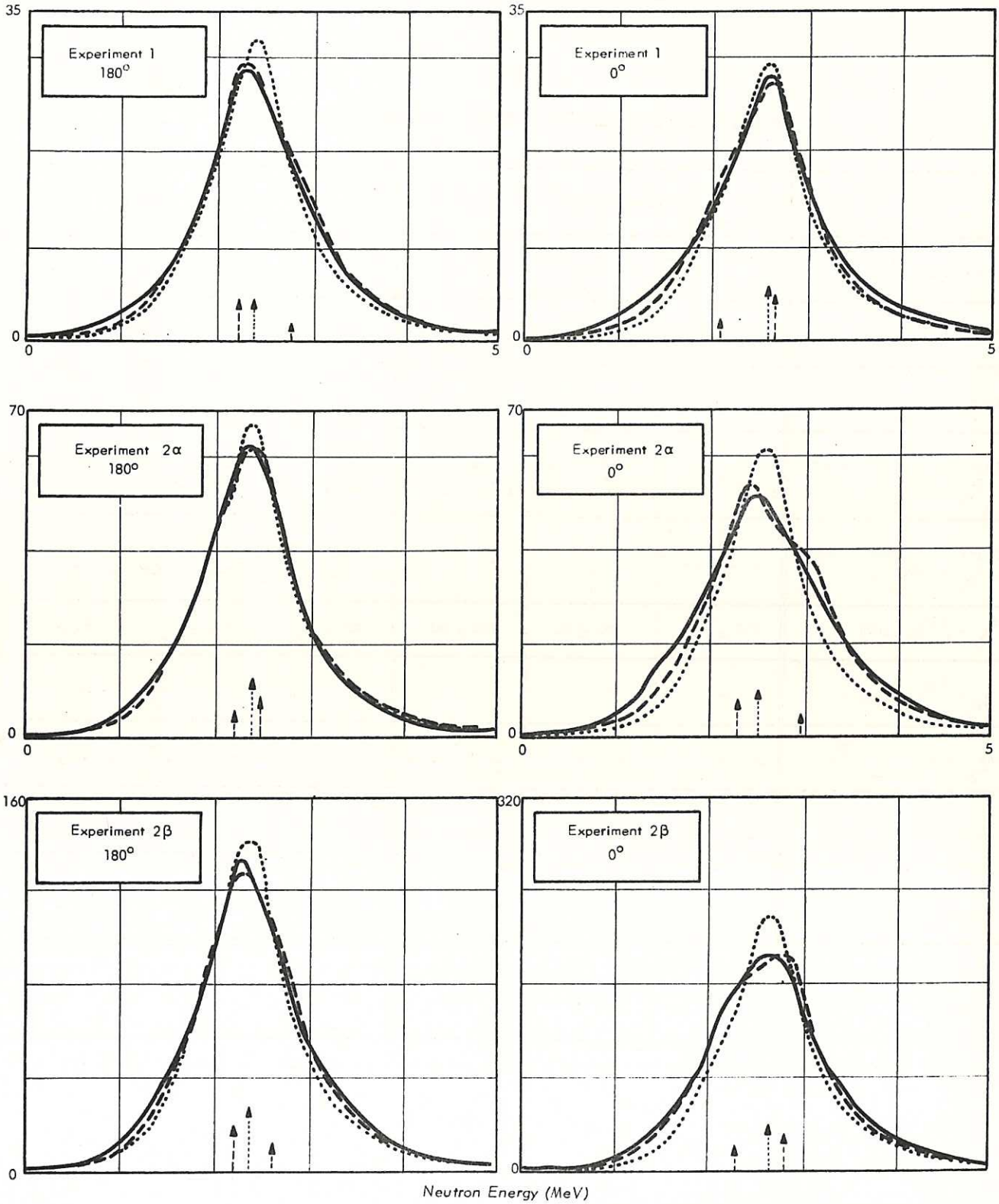

CLM-P 21 Fig. 5 Comparison of the observed spectra (axial) with the best fitting curves based on the one and two group models. The arrows indicate the positions and relative intensities of the monoenergetic lines which produce the fitted curves when broadened with the instrumental width.

TABLE 3.

TANGENTIAL RESULTS INTERPRETED IN TERMS OF ONE AND TWO-GROUP MODELS

	One-group model						Two-group model					
Experiment	1		2α		2β		1		2α		2β	
View	0°	180°	0°	180°	0°	180°	0°	180°	0°	180°	0°	180°
Number of tracks analysed	40	42	88	83	304	187	40	42	88	83	304	187
Position of line 1 (MeV) $^{o}E_1$ / $^{180}E_1$	2.56 ± 0.04	2.42 ± 0.04	2.56 ± 0.08	2.40 ± 0.02	2.62 ± 0.05	2.36 ± 0.04	2.64 ± 0.04	2.32 ± 0.02	2.36 ± 0.09	2.50 ± 0.03	2.80 ± 0.04	2.24 ± 0.04
Position of line 2 (MeV) $^{o}E_2$ / $^{180}E_2$	-	-	-	-	-	-	2.08 ± 0.14	2.83 ± 0.06	3.02 ± 0.09	2.22 ± 0.05	2.26 ± 0.08	2.64 ± 0.05
$^{o}E_1 - {}^{180}E_1$ (keV)	140 ± 53		160 ± 80		260 ± 60		320 ± 45		-140 ± 95		560 ± 50	
$^{o}E_2 - {}^{180}E_2$ (keV)	-		-		-		-750 ± 150		800 ± 110		-380 ± 90	
$^{*}V_{z1}$ (cm/sec x 10^{-7})	+3.1 ± 1.2		+3.5 ± 1.8		+5.7 ± 1.3		+7.1 ± 1.1		-3.1 ± 2.2		+12.3 ± 1.1	
$^{*}V_{z2}$ (cm/sec x 10^{-7})	-		-		-		-16.5 ± 3.3		+17.6 ± 2.3		-8.4 ± 2.0	
Relative neutron yield group 1 / group 2	-		-		-		4.0 ± 1.0		2.0 ± 0.4		1.9 ± 0.1	
Angle between B_{zo} and I_z	0°		180°		180°		0°		180°		180°	

$^{*}V_z$ the axial centre-of-mass velocity component, is positive when in the same sense as positive gas current

TABLE 4.

PROPERTIES OF THE OBSERVED PERPENDICULAR SPECTRA

Experiment	View	From Histograms			From Gaussian Addition Spectra		Mean of the best fitting theoretical spectra (MeV)
		Weighted Mean (MeV)	Standard Deviation (MeV)	Number of tracks	Position of Mode (MeV)	Full Width at half-height (MeV)	
2α	top-half	2.25 ± 0.10	0.29	18	2.28 ± 0.06	1.4 ± 0.3	-
	bottom-half	1.91 ± 0.11	0.65	14	2.35 ± 0.08	2.2 ± 0.5	-
	sum	2.09 ± 0.07	0.49	32	2.35 ± 0.05	1.7 ± 0.3	2.01
2β	top-half	1.99 ± 0.04	0.52	46	2.20 ± 0.04	2.1 ± 0.3	-
	bottom-half	2.01 ± 0.05	0.43	34	1.90 ± 0.05	1.8 ± 0.3	-
	sum	2.00 ± 0.03	0.48	80	2.05 ± 0.03	1.9 ± 0.2	2.02

TABLE 5.

COMBINED RESULTS FROM TANGENTIAL AND PERPENDICULAR SPECTRA

Experiment	Total centre-of-mass velocity (cm/sec)	Components of centre-of-mass velocity (cm/sec)		Deuteron energy (keV)
		Azimuthal	Radial	
2α	$(2.5^{+3.0}_{-1.5}) \times 10^8$	-	-	260
2β	$(2.9 \pm 0.9) \times 10^8$	$(1.5 \pm 0.9) \times 10^8$	$(2.3 \pm 1.5) \times 10^8$	350

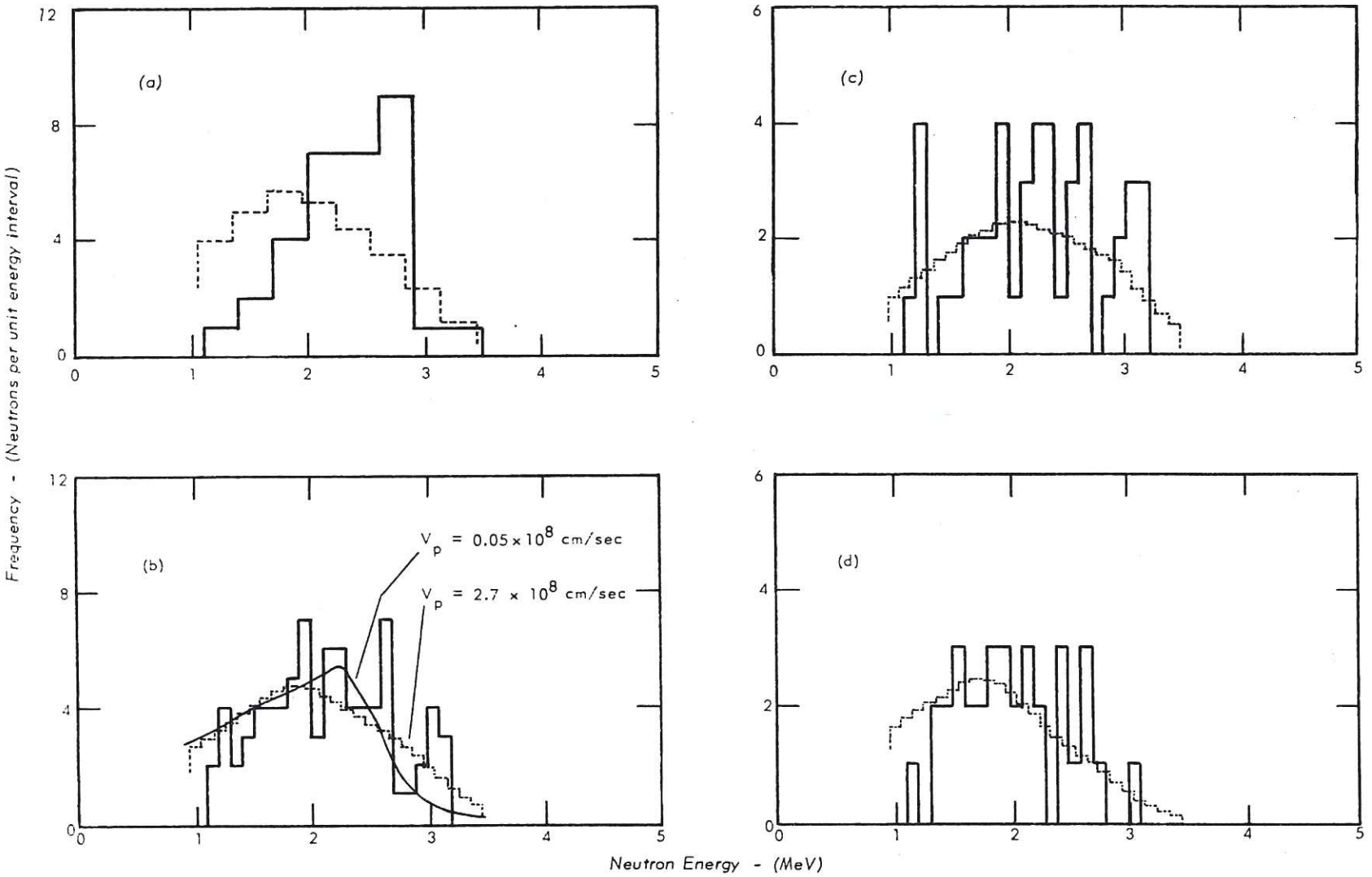

CLM-P 21 Fig. 6

The 'radial' spectra from Experiment 2, (a) 'sum spectrum', experiment 2α, (b) 'sum-spectrum', 2β, (c) 'top-half view', 2β, (d) 'bottom-half' view, 2β. Also shown are the best fitting theoretical spectra based on a one-group model and in (b) the theoretical spectrum from deuterons with $V_p \simeq 0$.

probability of fit of 0.70 for ν degrees of freedom.

21. In order to compare the one- and two-group models, a significance test must be applied to the various curves. A χ^2 test (KENDALL, 1945) is not applicable to the Gaussian addition curves because of the co-variance between adjacent points of the experimental curve. This test, was however, applied to the frequency histograms of experiment 2, the result being that the 2-group model gave a significance of 5 per cent whereas the one-group model gave less than 0.01 per cent significance. In these tests no allowance was made for the variation of accuracy of the observations. The very low value of the significance for the one-group model shows that it does not account satisfactorily for the experimental results. The value for the 2-group model, while still lower than would normally be required for accepting this interpretation, shows that this model represents a nearer approximation to the actual energy distribution. A higher significance could no doubt be obtained by taking more groups, or a continuous distribution, but such elaborate calculations are not warranted by the overall accuracy of the experimental data.

PERPENDICULAR SPECTRA

22. The experimental results are shown in the form of histograms in Figure 6 and the main features are given in Table 4. The most noticeable feature of these spectra is their greater width and lower mean energy when compared with the tangential results. It was obvious that a careful study of the neutron scattering involved is necessary before interpreting the spectra in terms of a finite velocity of centre-of-mass of the fusing deuteron system.

23. Neutrons scattered by the various components of ZETA shown in Figure 1 have a more dominating effect on the perpendicular energy spectra than on the tangential spectra because of the geometry and the greater bulk of material viewed in the former case. An estimate of the effect of scattering on a given incident neutron energy distribution was made by computing the scattered spectrum with a Monte Carlo method using a plane geometry approximation, with all the various components of the ZETA apparatus in the line of sight of the cloud chamber, taken into account.

24. The perpendicular spectra, in histogram form, were analysed by assuming all the fusing deuterons to have the same instantaneous values of radial and azimuthal centre-of-mass velocity components (one-group model). Purely radial motion of the deuterons would

give identical spectra from the top and bottom half views while azimuthal motion would introduce a difference between them. Hence, analysis of these spectra gives an estimate of the azimuthal component of the deuteron centre-of-mass velocity. The 'sum' spectrum (formed by adding the spectra from the top and bottom half views) gives the total perpendicular motion.

25. Theoretical spectra were calculated (WARD, 1962) for a range of values of V_r and V_o, the radial and azimuthal components of centre-of-mass velocity respectively. These were broadened by the computed effect of scattering and again with the measured instrumental width of the cloud chamber. The results were then compared with the observed spectra by applying a χ^2 test. The theoretical spectra which gave the mimimum value of χ^2 are shown superimposed on the experimental results in Figure 6, where the corresponding velocity values are also indicated. The resultant perpendicular velocity is given by $V_p^2 = V_\theta^2 + V_r^2$.

26. In experiment 2α there were not enough tracks detected to enable an estimate of the components of the perpendicular velocity to be made and in addition the probability of the experimental spectra being produced by the perpendicular deuteron velocity giving the most significant fit is only 1 per cent.

27. The spectra from experiment 2β show a 50 per cent probability of having been produced by deuterons with $V_p = 2.7 \times 10^8$ cm/sec and an 8 per cent probability of a source with zero perpendicular velocity. The 2β half view spectra are less definite and show corresponding probabilities of 20 per cent for $V_\theta = 1.5 \times 10^8$ cm/sec and 3 per cent for $V_\theta = 0$.

28. Combining the perpendicular velocities obtained above with the tangential velocities obtained in para. 17 et seq., expressing the result as a deuteron energy assuming target deuteron at rest, gives the values indicated in Table 5. The possible errors given for the total centre-of-mass velocity are the 70 per cent confidence limits and are dominated by the possible error in the perpendicular component. The latter is obtained from the rate, with respect to velocity, at which χ^2 approaches its mimimum.

4. DISCUSSION

29. The main features of the results, namely the apparently large perpendicular velocities and the tangential motion of deuterons both with and against the gas current, are self consistant, since fine pitch helical motion in a torus would give tangential spectra which, when interpreted in terms of cylindrical geometry of the source, would suggest the existence of two velocity groups of fusing deuterons.

30. A predomintly perpendicular motion of the ions implies that the deuterons gain their energy over distances of the order of a few discharge tube radii. If the ions had gained their energy over a series of circuits of the torus they would have predominantly azimuthal or tangential velocities. This suggests that the ions are not confined by the magnetic fields of the discharge. This result is consistent with the fact that in ZETA 3 MJ under the conditions of Experiment 2, the azimuthal magnetic field has a maximum value of $2.5 - 3.0 \times 10^3$ gauss at a distance of 15 cm from the discharge axis and the axial field a maximum value of $4.5 - 5.0 \times 10^3$ gauss at the axis. The Larmor radius of a 350 keV deuteron in fields of this order would be 25 - 50 cm.

31. The question now arises whether such high deuteron velocities are energetically possible. The energy required depends on whether the fusion reactions occur in the gas or on the walls.

32. Assuming first a uniform 'cold' ion density in the discharge of 2×10^{18} ions/cm^3 and a 'target' thickness of 50 cms, 10^{18} deuterons would have to be accelerated to an energy of 350 keV to give the observed yield of 5×10^7 neutrons per discharge under the conditions of Experiment 2β. The energy required for this would be approximately 50 kilojoules, one twentieth of the energy originally stored in the capacitor bank. This result is not precluded by the measurement of energy loss from ZETA (GIBSON and MASON, 1961). If, however, the fast ions are not confined, but impinge on deuterium absorbed into the torus walls (WEISBECK, 1960), a much smaller total energy is required. Assuming a constant flux of deuterons of M cm^{-2} eV^{-1} per discharge impinging on walls having a 1:1 atomic ratio of deuterium absorbed in the walls, the number of neutrons emitted per square centrimetre of the torus wall is given by:-

$$N = \frac{Mn}{dE/dx} \int_0^{E_{max}} \int_0^{E_1} \sigma(E)dE \; . \; dE_1$$

where N is the number of neutrons per square centimetre per discharge, taken as 1.4×10^2, n the deuterium atomic density in the wall, taken as 1.6×10^{23} cm^{-3}, $\frac{dE}{dx}$ is the rate of loss of deuteron energy in the wall and is assumed constant at 2×10^6 keV cm^{-1}, $\sigma(E)$ is the d-d fusion cross-section, E the deuteron energy and E_{max} the maximum of E, i.e. 350 keV. The result of such an integration gives M = 300 deuterons cm^{-2} eV^{-1} $discharge^{-1}$. This represents an energy content of about 2 joules in the fast ions.

33. Evidence that the neutrons are mainly produced at the walls is given by the observed ratio of the number of neutrons detected by the tangential view to those detected by the perpendicular view. The expected ratio is 0.9 for a wall source and 2.0 for a volume source. These theoretical ratios include approximate corrections for scattering effects. The observed ratio was 0.72 ± 0.01. On the other hand, previous experiments (HARDING et al., 1958 and ROSE et al., 1958) gave results which favoured a volume source. However these experiments were performed under conditions which did not produce catastrophic 'pump-out' during the main discharge and the results are not strictly comparable with those of experiment 2β.

34. To accelerate deuterons up to 350 keV within a few circuits of the perpendicular plane, continuous forces equivalent to electric fields of between 500 V/cm and 5kV/cm would be required. Such large forces could arise from polarization of the plasma produced by electrostatic instability or other co-operative phenomena. Alternatively, a travelling wave could provide the necessary acceleration mechanism. These mechanisms require electric fields in the plasma to be perpendicular to the magnetic field. Such fields can exist and have been observed in ZETA (GIBSON and MASON, 1961) although the measured strengths average only about 50 V/cm.

35. It is of interest to compare these results with those obtained on other machines. Recent results (AFROSIMOV et al., 1960) from the toroidal pinch device ALPHA (which has dimensions and characteristics very similar to those for ZETA) indicate the presence of neutral hydrogen atoms ejected from the discharge with energies of thousands of electron volts. The value of deuteron flux in ZETA, obtained by assuming fusion at the torus walls, is compared with the hydrogen atom flux to the walls obtained by the Russian workers in Fig.7. This suggests that the flux of ions with sufficient energy to escape from the

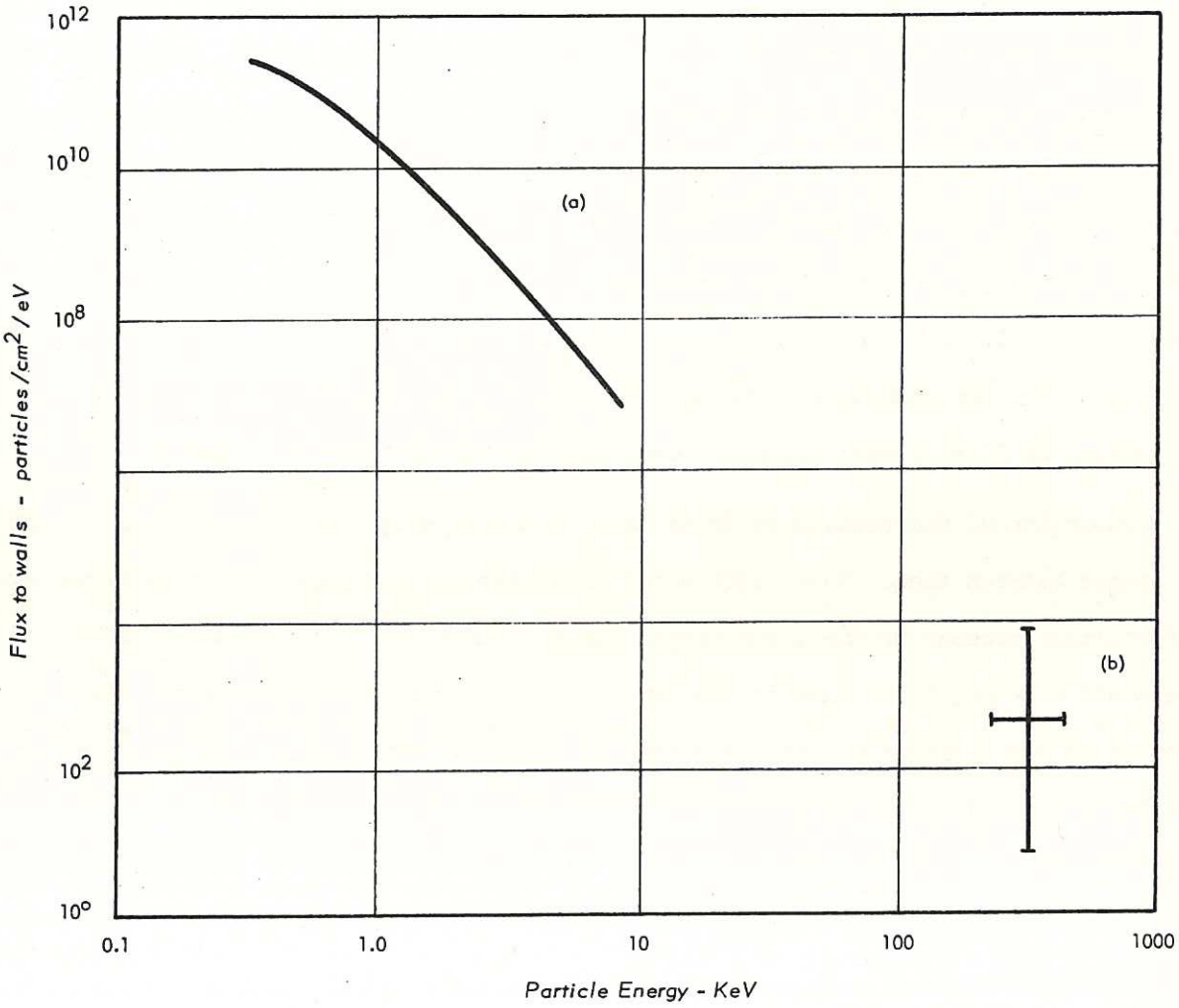

CLM-P 21 Fig. 7

(a) The flux of neutral hydrogen atoms to the wall of ALPHA obtained by Afrosimov et al. (1960) with the initial discharge conditions. Capacitor bank potential $V_c = 15$ kV, B_z = 360 gauss and a pressure of 0.2 m torr hydrogen.

(b) The flux of high energy deuterons to the wall of ZETA estimated from the observed energy and yield of the emitted neutrons, assuming that the neutrons are produced at the wall. Initial discharge conditions V_c = 15 kV, B_z = 1,100 gauss, pressure = 0.3 m torr deuterium.

ZETA discharge is consistent with the flux of atoms leaving ALPHA and infers that the energy distribution of ions and atoms in the plasma volume are similar to each other, in agreement with the prediction of AFROSIMOV et al., (1960). A further point for comparison of the two devices is in the variation of the neutral particle flux from ALPHA and the neutron yield of ZETA, both increasing as capacitor bank potential increases and as initial axial magnetic field or gas pressure decreases.

36. Measurement of the proton energies from SCEPTRE III (JONES et al., 1961) has shown the presence of deuterons with energies up to 12 keV travelling in a predominantly axial direction. The radial component of the centre-of-mass velocity of the high energy deuterons is only 2×10^7 cm/sec. This value is much less than that obtained by scaling down the continuous electric field necessary to produce ions of the energy found in ZETA. An electric field of 500 V/cm could accelerate ions up to 350 keV in ZETA within a few circuits of the perpendicular plane and up to 90 keV over the SCEPTRE radius of 15 cm. The protons in SCEPTRE were found to come from reactions within the plasma.

37. Comparison of the results of Experiment 2α and 2β shows that there is no significant difference between them. Such differences as appear in the tangential results may easily be fortuitous because of the large perpendicular velocities. The mechanism of deuteron acceleration could be the same in the two types of discharge, the increased yield of neutrons in the β-type could be due either to a larger number of ions accelerated or a greater time duration of the acceleration process. Alternatively, escape of the deuterons from the magnetic confining fields in the β-discharge and fusion in the deuterium dense wall target would give a greater neutron yield than the fusion of ions confined within the α discharge.

5. CONCLUSIONS

38. Experiments 1 and 2α are consistent with the conclusions of previous authors, working both on ZETA and on other toroidal discharge devices, that the neutrons do not arise from a stationary thermonuclear plasma, but are probably due to a small number of deuterons accelerated to high energies by electric fields. Experiment 2β confirms the above conclusions and although the nature of the ion acceleration mechanism is still unknown, an important clue is suggested, namely that the deuterons could be accelerated mainly in a radial direction and to much higher energies (300 keV) than was previously known.

ACKNOWLEDGEMENTS

39. The authors would like to thank the Reactor Physics Department of the University of Birmingham for the extended loan of the cloud chamber. Thanks are also due to P.O. Hawkins, J.D.L.H. Wood, R. Bottomly and E.W. Saker of S.E.R.L. Baldock for the loan of the d-d tube, and for their assistance with its operation. E.K. Sinton designed and constructed the electronics for the d-d tube.

40. Invaluable assistance has been given by Miss J. Masters and E.J. York of the Theoretical Physics Division who wrote many of the programmes necessary for the computation involved in the analysis, and by B.E. Cooper who gave advice on the statistical problems which arose. We are grateful to the ZETA Operations Staff for their co-operation, to J.B. Parker of A.W.R.E. Aldermaston for performing the neutron scattering calculations on their IBM 7030 computer and to P.G. Dawson, K.J. Hopkins and P.J. Brazier who assisted with the experiments and undertook much of the photograph scanning.

41. The guidance and advice of G.N. Harding is much appreciated as are the many helpful discussions with R.S. Pease and other members of Culham Laboratory Staff.

42. One of us (P.A.C.) held a maintenance grant from the English Electric Company at Birmingham University during the course of the experiment and would like to thank Dr. J. Walker (Birmingham) and Dr. E. Robinson (English Electric) for their assistance and advice.